

MEASUREMENT OF INDUCTION MOTOR SPEED  
FROM INDUCED SLIP FREQUENCY SIGNAL

by

CAI, JI-YUAN

A THESIS SUBMITTED IN PARTIAL FULFILMENT OF  
THE REQUIREMENT FOR THE DEGREE OF

MASTER OF APPLIED SCIENCE

in the Department of  
Electrical Engineering

We accept this thesis as conforming to the  
required standard

Research Supervisor  
Members of the Committee.

per Head of the Department

Members of the Department  
of Electrical Engineering  
THE UNIVERSITY OF BRITISH COLUMBIA

December, 1985

© Cai Ji-Yuan, 1985

In presenting this thesis in partial fulfilment of the requirements for an advanced degree at the University of British Columbia, I agree that the Library shall make it freely available for reference and study. I further agree that permission for extensive copying of this thesis for scholarly purposes may be granted by the head of my department or by his or her representatives. It is understood that copying or publication of this thesis for financial gain shall not be allowed without my written permission.

Department of \_\_\_\_\_

The University of British Columbia  
1956 Main Mall  
Vancouver, Canada  
V6T 1Y3

Date \_\_\_\_\_

## ABSTRACT

A method to detect the slip of a three-phase or single-phase induction motor and hence determine the motor speed is proposed. A pick-up coil is placed in close proximity to the motor and by suitable amplification and filtering of the weak slip frequency signal, the slip frequency signal component is isolated for the speed measurement. No device needs to be attached to the motor shaft.

Experimental results from four test induction motors show that the proposed method of speed measurement is fully feasible and applies to normal loads, i.e., for slip less than 13% with considerable accuracy. Therefore, even the speed of sealed induction motor such as those used in refrigerators can be easily measured.

## TABLE OF CONTENTS

	Page
ABSTRACT .....	ii
TABLE OF CONTENTS .....	iii
LIST OF ILLUSTRATIONS .....	iv
LIST OF TABLES .....	v
ACKNOWLEDGEMENT .....	vi
1. INTRODUCTION .....	1
1.1 General .....	1
1.2 Principle of Operation and Performance Equation of Induction Motors .....	1
1.3 Previous Method of Slip Frequency Measurement .....	4
1.4 Proposed Method of Slip Frequency Measurement .....	4
2. FEASIBILITY TEST OF SPEED MEASUREMENT TECHNIQUE .....	6
2.1 Description of Measurement and Circuit .....	6
2.2 Calculation of Slip Frequency $f_s$ .....	7
2.3 Measurement of Supply Frequency .....	8
2.4 Experimental Results .....	8
3. CONSTRUCTION OF SPEED MEASUREMENT CIRCUIT .....	14
3.1 The Overall Slip Frequency Measurement Circuit .....	14
3.2 Inductive Device Choke .....	18
3.3 Second Order Butterworth Low-Pass Filter .....	18
3.4 Input Buffer and Attenuator .....	22
3.5 Phase Shifter .....	23
4. EXPERIMENTAL RESULTS .....	25
4.1 Discussion of Experimental Results .....	36
4.2 Supply Frequency Signal Component .....	39
4.3 Measurement of Pole Pairs .....	39
5. CONCLUSION .....	43
REFERENCES .....	44
APPENDICES .....	46
A1. Derivation of the Frequency Response Equation for Second Order Butterworth Low-Pass Filter .....	46
A2. Calculation of Slip Frequency Signal Component .....	49

## LIST OF ILLUSTRATIONS

Figure	Page
2.1 Signal Pickup and Detection with Choke and Galvanometer .....	6
2.2 Equivalent Circuit of Figure 2.1 .....	7
2.3 Slip Frequency Waveform of Motor m1.....	10
2.3 Slip Frequency Waveform of Motor m2.....	10
2.5 Supply Frequency Waveform of Motor m1.....	10
2.6 Supply Frequency Waveform of Motor m2.....	10
2.7 Speed Comparison .....	12
3.1 Overall Block Diagram of Slip Frequency Measurement .....	15
3.2 Circuit Components .....	16
(a) Phase Shifter .....	16
(b) Choke .....	16
(c) Phasor Diagram of Phase Shifter .....	16
(d) Input Buffer $G_1$ .....	16
(e) Attenuator $G$ .....	16
(f) Second Order <sup>a</sup> Butterworth Low-Pass Filter Stage (each of them from Filter 1 to Filter 6) .....	16
4.1 Experimental Setup .....	26
4.2 Comparison of Expected and Detected Slip Frequency for Induction Motor (a) M1 (b) M2 (c) M3 (d) M4 .....	38
4.3 Amplitude Ratio of 60 Hz Supply Frequency Signal to Slip Frequency Signal .....	40
4.4 Location Diagram of Pole Pairs Measurement .....	41
4.5 Choke Voltage Waveform at Several Locations .....	41
(a) Supply Frequency Reference Waveform .....	41
(b) at $L_1$ (c) at $L_2$ (d) at $L_3$ .....	41
A1.1 Second Order Butterworth Low-Pass Filter .....	46
A2.1 Gain Curve of Three Identical Second Order Butterworth Filter Stages in Cascade .....	50

## LIST OF TABLES

Table	Page
2.1 Specification of Motors and Instruments .....	9
2.2 Measured Values at No Load .....	10
2.3 Measurement Results .....	11
3.1 Specification of Circuits in Figure 3.2 .....	17
4.1 Motor Specifications .....	25
4.2 Experimental Results of Motor M1 .....	27
4.3 Experimental Results of Motor M2 .....	29
4.4 Experimental Results of Motor M3 .....	31
4.5 Experimental Results of Motor M4 .....	33
4.6 Waveform Evaluation of Detected Slip Frequency .....	37
A2.1 Calculated $G_{\text{NodB}}$ ( $N \leq 3$ ) .....	52
A2.2 Calculated $G_{\text{NodB}}$ ( $N > 3$ ) .....	54

## ACKNOWLEDGEMENT

I wish to express my deepest gratitude to my supervisor, Dr. Malcome Wvong for his valuable assistance, constant encouragement and correct guidance in my graduate program and the preparation of this thesis.

I sincerely wish to thank my wife, Hui Chun, for the cooperation, understanding and encouragement during the entire period of the study.

## 1. INTRODUCTION

### 1.1 General

One of the most important trends in variable speed drives is the use of induction motors. This technique has been studied in recent years [1-6], because the induction motor can be used in a variety of poor working conditions and at less expense than dc machines. It is widely used in ac drives with constant speed requirements. Great progress in thyristor and power-transistor inverter design has made it possible to use induction motors in variable-speed drive systems. High performance of induction motor drives can be obtained by complex loop control systems, such as slip frequency control [2-4], flux control [2-4], and vector control or phase-locked loop [pLL] control [5,6].

But the parameter of rotating speed must be available as a measurement for these control systems. Conventional speed measurement requires a tachometer, transducer or device to be attached to the motor shaft. There would be less installation and maintenance costs if speed could be measured without shaft attachment of any such gadget.

### 1.2 The Principle of Operation and Performance Equation of Induction Motors

Some important aspects of induction motors will be briefly reviewed here. As we know, there are two kinds of ac motors, namely, synchronous and asynchronous motors, the latter being more commonly known as induction motors. Induction motors are widely used in ac drive systems because of low capital and maintenance costs.

The principle of operation of an induction motor is different from that of a synchronous motor which has a speed always equal to the synchronous speed produced by a rotating magnetic field. When three phase voltage

is applied to the stator of a three phase induction motor, a rotating magnetic field exists in the space, at a angular speed corresponding to the supply frequency and cuts the rotor windings. Current flows in the short-circuited rotor windings, and sets up a rotating magnetic field which interacts with the stator field. The torque produced results in rotation of the motor rotor. With motion the current in the rotor is at a frequency which reflects the relative movement of the rotor with respect to the rotating magnetic field set up by the stator windings. If a signal corresponding to the frequency of the rotor current can be picked up in the vicinity of the motor then the speed of the motor can be readily determined.

Indeed, the speed of the motor will never reach the speed of the rotating magnetic field set up by the stator, the so-called synchronous speed. The speed of the induction motor depends upon the motor size, mechanical load, etc. Usually, for rated load for most induction motors, the speed range is from 99% to 92% of synchronous speed (i.e. rotor current frequency is 0.6 Hz to 5 Hz for 60 Hz motors).

In order to calculate the motor speed by measuring rotor current frequency, the relations among induction motor parameters need to be reviewed.

slip  $s$  is defined as follows:

$$s = \frac{n - n_1}{n} \quad (1.1)$$

where  $n$  is synchronous speed.

$n_1$  is rotor speed, i.e. asynchronous speed.

The rotor rotates at asynchronous speed such that the slip frequency is given by

$$f_s = sf \quad (1.2)$$

where  $f_s$  is slip frequency

$f$  is supply frequency.

The frequency of rotor current is at slip frequency. It is obvious that if  $s = 1$  the motor stays at rest because the rotating magnetic field cuts the rotor at synchronous speed corresponding to the supply frequency. The slip can never be zero because the rotor would need to run at synchronous speed and this would not be possible because no voltage would be induced in the rotor.

Substituting (1.1) into (1.2) we get:

$$f_s = \frac{n-n_1}{n} f \quad (1.3)$$

since  $60f$

$$n = \frac{60f}{p} \quad (1.4)$$

where  $p$  is the number of pole pairs.

Eliminating  $f$  in (1.3) and (1.4)

$$f_s = (n-n_1) \frac{p}{60} \quad (1.5)$$

and eliminating  $n$  in (1.3) and (1.4)

$$n_1 = \frac{f-f_s}{p} 60 \quad (1.6)$$

If supply frequency  $f = 60$  Hz then eqn. (1.6) becomes

$$n_1 = \frac{1}{p} (3600 - 60 f_s) \quad (1.7)$$

Let  $N = 60 f_s$  (1.8)

or  $f_s = \frac{N}{60}$  (1.9)

then  $n_1 = \frac{1}{p} (3600 - N)$  (1.10)

Here  $N$  is the frequency of the signal which will be found in the simple experiment discussed in chapter 2.

From (1.6) derived above, actual motor speed can be determined through measurement of slip frequency,  $f_s$ , the given supply frequency,  $f$  and the number of pole pairs,  $p$ .

### 1.3 Previous Method of Slip Frequency Measurement

Ishida, M. and Iwata, K. (7) and (8) have proposed the use of rotor slot harmonics to determine the slip frequency of induction motors. The air-gap flux of an induction motor when fed by a balanced sinusoidal power supply contains the space harmonics, due to variation of reluctance of the rotor and stator slots and to spatial distribution of stator windings. The influence of stator slots to harmonics in stator voltage can be neglected in comparison with that of rotor slots. Thus, when the motor is operating each stator winding contains both components of the fundamental and slot harmonic voltages. The detection of the slot harmonics can be obtained by the use of three single-phase transformers. The primary of each single-phase transformer is connected in parallel to each stator winding and all the secondary windings of the transformer in series for output. The slip frequency  $f_s$  can be detected only for motors with the number of rotor slots equal to  $3n \pm 1$  for  $n = 1, 2, 3, \dots$ , reported by the authors. Experimental results show good linearity of slip frequency measured by the proposed method with respect to that measured by conventional means in the range of slip frequency up to +30% of the stator frequency. However, this method can only be used where the number of the rotor slots per pole pair is known and is equal to  $3n \pm 1$ .

### 1.4 Proposed Method of Slip Frequency Measurement

In this thesis a different method of slip frequency measurement of an induction motor and hence its speed will be reported. By the use of

an inductive pick-up coil in the vicinity of the induction motor it is found that only two major signal components, namely, the supply frequency (60 Hz) and the slip frequency ( $f_s$ ), exist in the inductive choke voltage. Even though there is very poor signal to noise ratio, for the slip frequency signal with respect to the supply frequency, the supply frequency ("noise") signal can be filtered out. The unique slip frequency,  $f_s$ , can then be detected to determine the motor speed. The method does not require the attachment of any device to the motor shaft and the number of rotor slots to be known, etc. Therefore, it offers the measurement of the induction motor for more convenience.

The thesis project is aimed at investigating this concept of using the slip frequency component of leakage flux available in the field around an induction motor to determine the motor speed. However, the optimization of the inductive pick-up transducer, filter stages and the display of the speed signal is not attempted in this thesis.

A simple experiment to check the feasibility of the proposed method is discussed in chapter 2. The result of that experiment guided the design of the final speed measurement circuit, details of which are given in chapter 3. Finally, test results for four induction motors are given and discussed in chapter 4.

## 2. FEASIBILITY TEST OF SPEED MEASUREMENT TECHNIQUE

To test the feasibility of the speed measuring technique, a simple experiment was done using an inductive pick-up coil and a galvanometer. The experiment will indicate two important points, namely;

- (1) The slip frequency signal  $f_s$  exists in the space around the motor when it is running.
- (2) The slip frequency signal together with a strong signal at the supply frequency, 60 Hz, would be picked up by an inductive device, such as a choke and could be detected after suitable filtering.

### 2.1 Description of Measurement and Circuit

The circuit diagram of signal pick-up and detection is shown in Fig. 2.1. The choke is placed beside the motor in order to pick up the signal from the rotor circuit of the motor. High inductance and appropriate volume in the choke would be best. The inductive voltage in the choke (called choke voltage in this thesis) is indicated in the circuit by the galvanometer, which is highly sensitive to dc or low frequency

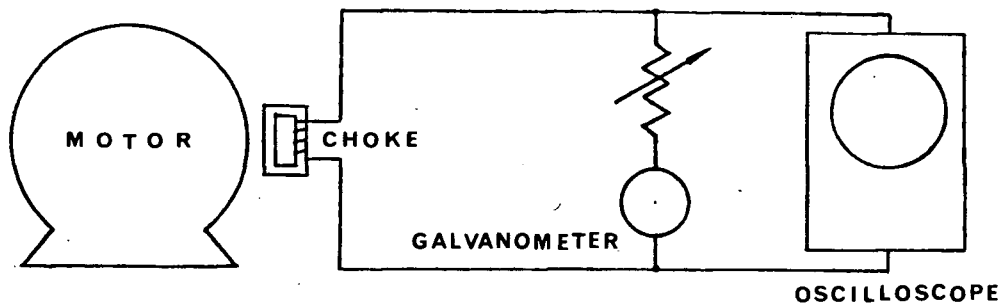


Fig 2.1 Signal Pickup and Detection with Choke and Galvanometer

current. The current value is determined by the deviation of the light spot on the scaled glass. The galvanometer also plays the role of a mechanical low-pass filter because its mechanical inertia will only allow it to follow the dc or low frequency signal and cuts off higher frequency signals, such as that of the supply frequency 60 Hz. The signal component of supply frequency may be measured and displayed on the oscilloscope by connecting the leads of the choke directly to the input of the oscilloscope.

## 2.2 Calculation of Slip Frequency $f_s$

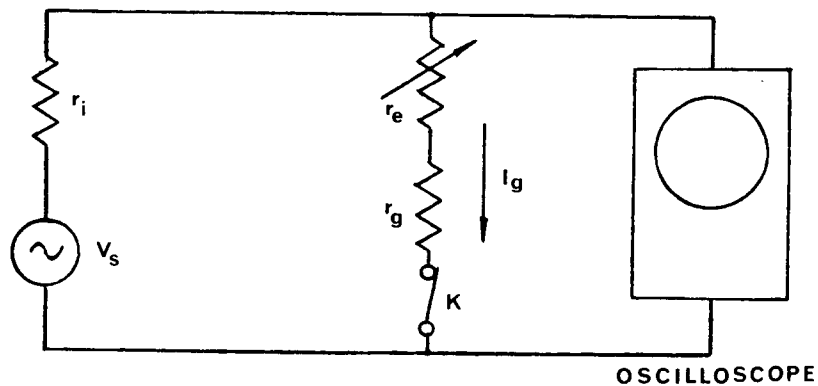


Fig 2.2 Equivalent Circuit of Fig 2.1

The equivalent circuit to measure the slip frequency  $f_s$  and its amplitude produced by rotor current is shown in Fig. 2.2 where

$r_i$  : choke resistance

$r_g$  : galvanometer resistance

$r_e$  : external variable resistance

$V_s$  : slip frequency voltage component in choke

Its amplitude  $V_s$  can be derived as follows

$$\text{We have } f_s = \frac{N}{60} \quad (1.9)$$

$$\text{Also } V_s = I_g (r_i + r_e + r_g) \quad (2.1)$$

The current  $I_g$  in eqn. (2.1) is given by

$$I_g = A_s \cdot sg \quad (2.2)$$

where  $A_s$  is the amplitude of the light spot deflection of the galvanometer and  $sg$  is the galvanometer sensitivity.

$$sg = 0.0035 \times 10^{-6} \text{ a.}$$

Substituting (2.2) into (2.1)

$$V_s = A_s \cdot sg (r_i + r_e + r_g) \quad (2.3)$$

In the experiment the slip frequency  $f_s$  is obtained by counting the number of oscillations  $N$  of the galvanometer light spot for one minute.

### 2.3 Measurement of supply frequency

The strong rotating magnetic field exists in the space around the motor when it is running so that the supply frequency 60 Hz is also induced in the choke. If the switch  $K$  is opened so that the choke voltage is applied directly to the input of the oscilloscope, as indicated in Fig. 2.2, the wave form on the oscilloscope indicates 60 Hz frequency and its amplitude which can be read from the scale. Even though the choke voltage contains both signal components of slip frequency and supply frequency 60 Hz, they are far enough apart and the supply frequency signal is much stronger than the slip frequency signal, that the wave form of supply frequency is hardly distorted at all.

### 2.4 Experimental Results

Measurements were carried out on two single-phase induction motors at no load. The specification of motors and instruments employed is shown in Table 2.1. The measurement, wave form and results are given in the

Tables and Figures as follows:

- (1) Table 2.2 shows the measured signal components of slip and supply frequencies.
- (2) Figure 2.3 and Figure 2.4 show the slip frequency wave forms for the two motors.
- (3) Figure 2.5 and Figure 2.6 show the supply frequency wave form seen on the oscilloscope.
- (4) Table 2.3 shows the final results for  $f_s$ ,  $n_1$ ,  $V_s$ ,  $V_{60}$  and

$$\frac{V_{60}}{V_s}.$$

Table 2.1 Specification of Motors and Instruments

Motor				choke		galvanometer	
	Pole Pairs P	Phase	Power (Hp)	$r_1$ ( $\Omega$ )	L (H)	Sens. Sg (a/mm)	$r_g$ ( $\Omega$ )
m1 (Motor1)	2	1	1/3	92	18.9	$3.5 \times 10^{-9}$	25
m2 (Motor2)	1	1	1/40	92	18.9	$3.5 \times 10^{-9}$	25

Table 2.2 Measured Values at no Load

Motor	Actual Speed Stroboscope (rpm)	Slip Frequency Component		Circuit			Supply Frequency Component	
		Frequency (N/min)	Amplitude $A_s$ (mm)	$r_i$	$r_e$	$r_g$	Frequency $f_{60}$ (Hz)	Amplitude $V_{60}$ (v. pk-pk)
				$(\Omega)$				
		Galvanometer					Oscilloscope	
m1	1792	16	48	92	330	25	60.5	1.2
m2	3495	105	10	92	3300	25	59.7	1.83
	3490	110	10	92	3300	25	59.7	1.83
	3486	114	10	92	3300	25	59.7	1.83

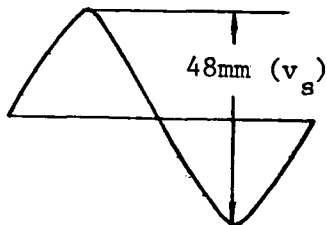


Fig 2.3 Slip Frequency Waveform of Motor m1

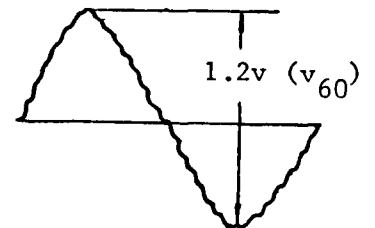


Fig 2.5 Supply Frequency Waveform of Motor m1

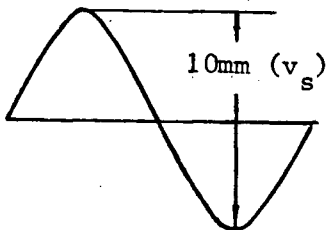


Fig 2.4 Slip frequency Waveform of Motor m2

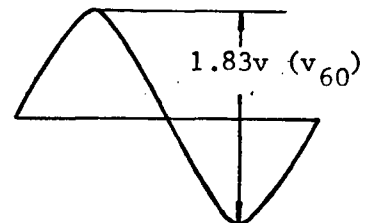


Fig 2.6 Supply Frequency Waveform of Motor m2

Table 2.3 Measurement Results

Motor	Actual Speed Stroboscope $n'$ (rpm)	Slip  S	Measured Components				Ratio $V_{60}/V_s$
			Slip Frequency $f_s$ (Hz)	Motor Speed $n_1$ (rpm)	Slip Frequency Voltage $V_s$ (v)	Supply Frequency Voltage $V_{60}$ (v)	
			Galvanometer		Oscilloscope		
m1	1792	0.44%	0.26	1792	$75 \times 10^{-6}$	1.2	$16 \times 10^3$
m2	3495	2.91%	1.75	3495	$119 \times 10^{-6}$	1.83	$15.3 \times 10^3$
	3490	3.05%	1.83	3490.2	$119 \times 10^{-6}$	1.83	$15.3 \times 10^3$
	3486	3.16%	1.90	3486	$119 \times 10^{-6}$	1.83	$15.3 \times 10^3$

The following indicates sample calculation for motor  $m_1$  using the measurements and values of Tables 2.1 and 2.2. From eqn. (1.9), (1.10) and Table 2.2

$$f_s = \frac{N}{60} = \frac{16}{60} = 0.26 \text{ Hz} \quad \text{with } p = 2$$

$$n_1 = \frac{1}{p} (3600 - 60 f_s) = \frac{1}{2} (3600 - 60 \times 0.26) = 1792 \text{ rpm.}$$

From eqn. (2.3) and Tables 2.1 and 2.2, the amplitude of slip frequency voltage is

$$V_s = A_s \cdot S_g (r_i + r_e + r_g)$$

$$S_g = 3.5 \times 10^{-9} \text{ a/mm}$$

$$r_i = 92 \Omega \quad r_e = 330 \Omega \quad r_g = 25 \Omega$$

$$\text{and } A_s = 48 \text{ mm} \quad p = 2$$

$$\text{So } V_s = 48 \times 3.5 \times 10^{-9} (92 + 330 + 25) = 75 \times 10^{-6} \text{ v.}$$

From Table 2.3 the actual speed  $n_1'$  measured by a stroboscope as compared with the speed  $n_1$  measured by the arrangement of choke and galvanometer are drawn in Fig. 2.7. any point on the straight

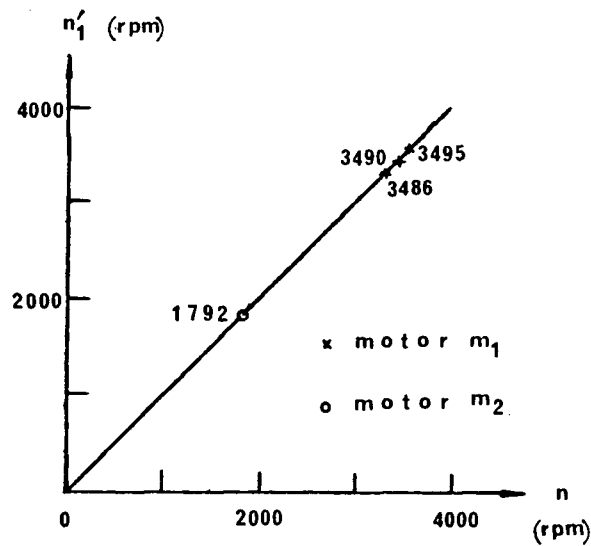


Fig 2.7 Speed Comparison

line means that the measured speed is equal to actual speed. The measured values of Table 2.3 agree exactly.

From the above results some important points can be made:

- (1) The speed as calculated using the oscillation per minute of the galvanometer light spot are identical with those measured with a stroboscope, which is generally acceptable as accurate speed measurement. So the proposed method will correctly determine the induction motor speed at no load.
- (2) There exists multiple frequency signal components in the field around the motor when it is operating. Obviously, the choke voltage will contain at least the signal components of supply frequency 60 Hz and slip frequency  $f_s$  that are related to the motor speed. From Table 2.3 it can be estimated that the range of  $f_s$  for the induction motors varies from 0.25 Hz at no load up to 5 Hz, i.e. that the speed range from 1792 rpm down to 1650 rpm for a four-pole motor.

(3) The amplitude ratio of  $V_{60}$  to  $V_s$  reaches up to  $16 \times 10^3$  approximately for motor  $m_1$ . The amplitude of supply frequency component  $V_{60}$  is much greater than the amplitude of the slip frequency component. Therefore, a multi-stage filter with amplification has to be designed to isolate the weaker slip frequency component  $V_s$  from the much stronger supply frequency signal component  $V_{60}$ .

(4) The determination of the motor speed not only depends upon the measured  $f_s$  but the synchronous speed has to be known i.e. the number of pole pairs for the motor has to be known. The equation (1.6) exhibits this relation

$$n_1 = \frac{60}{p} (f - f_s)$$

The number of pole pairs may be determined experimentally or from nameplate specification. This parameter  $p$  will be assumed to be given for the speed determination.

It is to be noted that the error of the slip frequency amplitude will increase with frequency because of the mechanical inertia of galvanometer. So the galvanometer can be considered as a mechanical low-pass filter with low corner frequency.

### 3. CONSTRUCTION OF SPEED MEASUREMENT CIRCUIT

The simple experiment described in chapter 2 demonstrated the feasibility of the technique to measure the speed of an induction motor by use of the slip frequency signal present the magnetic field around the motor. But the simple measurement set up using a galvanometer is limited in its ability to measure the whole range of speeds with varying load for different kinds of induction motors. Therefore, a more sophisticated filter circuit needs to be designed to replace the mechanical filter represented by the galvanometer.

Major factors to be considered in the circuit design are:

- (1) The measurement circuit is to use an active filter, with operational amplifiers as the active elements, and with multi-stage filtering. Each filter stage should attenuate the supply frequency signal and amplify the weak slip frequency component.
- (2) Each filter stage should work within the linear range of the operational amplifier i.e. within  $\pm 13$  volts
- (3) For the detection of the slip frequency for various motors, the multi-stage filter circuit should provide output at each stage because the number of filter stages needed varies with the type of induction motors and their speed.
- (4) The amplitude of the detected slip frequency can also be calculated through the multi-stage filter.

#### 3.1 The Overall Slip Frequency Measurement Circuit

The overall circuit is shown in Figure 3.1 and comprises the following:

- (1) Signal pickup i.e. inductive device, choke
- (2) Second order Butterworth low pass filter
- (3) Input buffer and attenuator
- (4) Alternative supply frequency phase shifter

The detailed circuits for each of the above are shown in Figure 3.2.

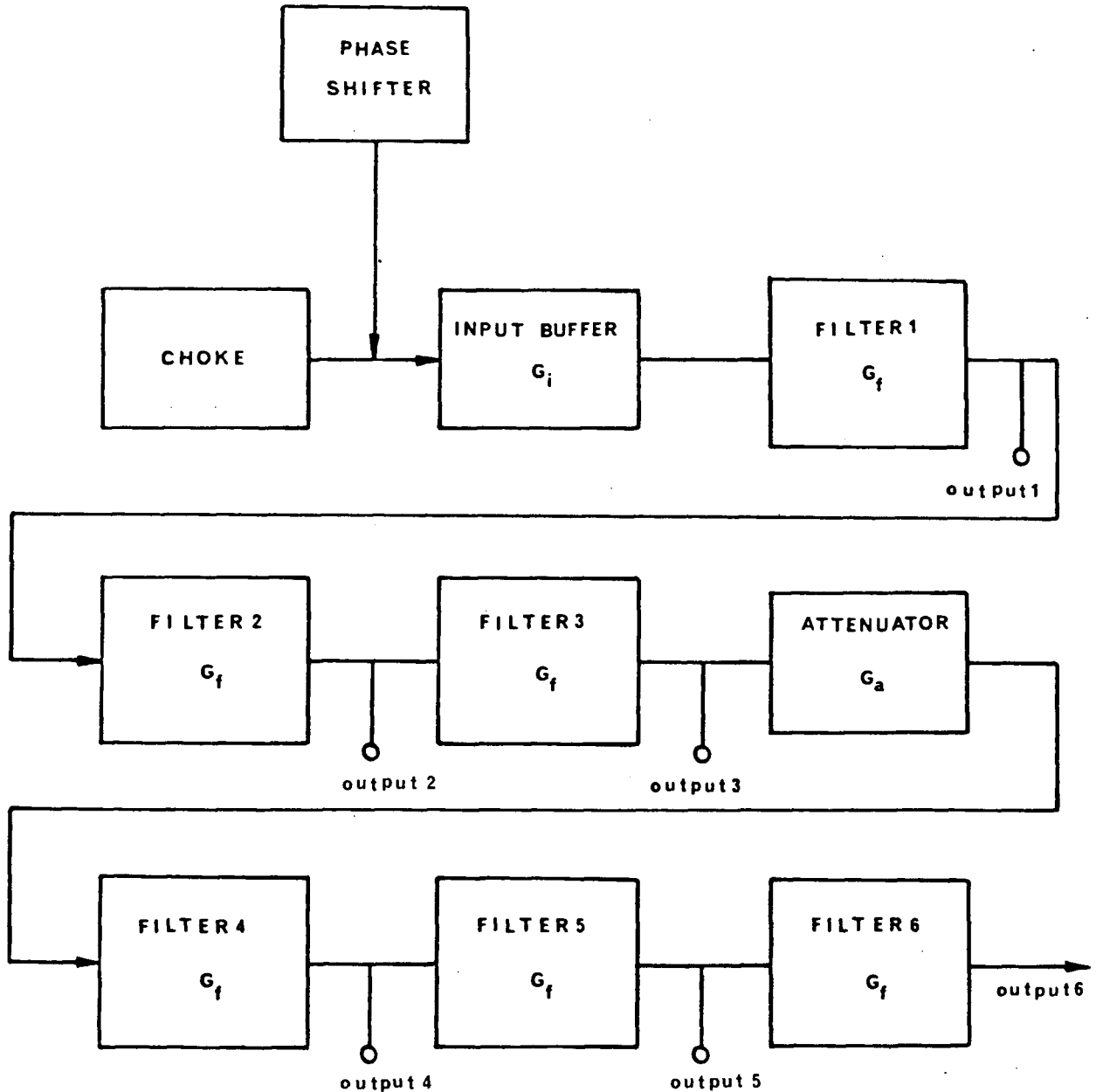


Fig 3.1 Overall Block Diagram of Slip Frequency Measurement

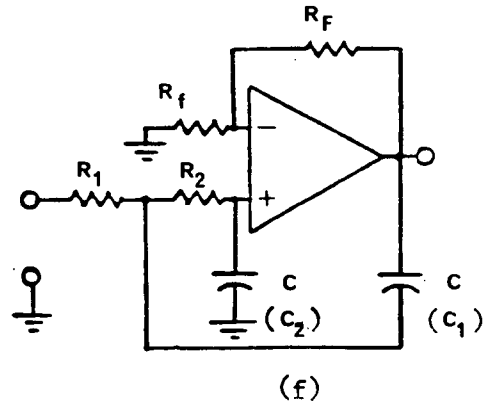
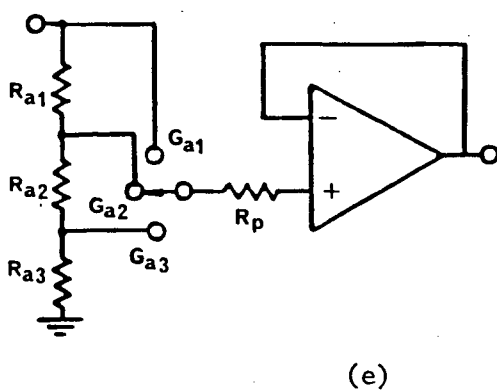
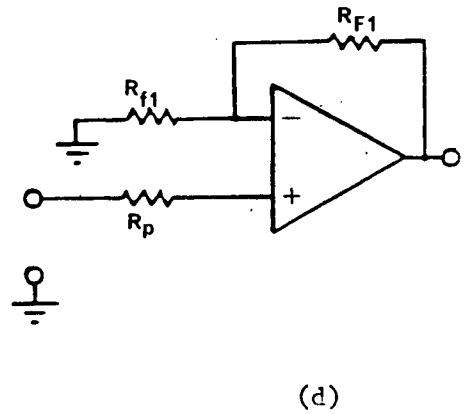
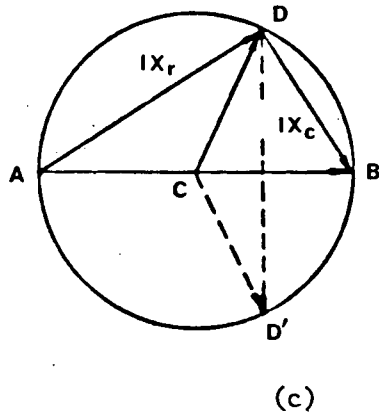
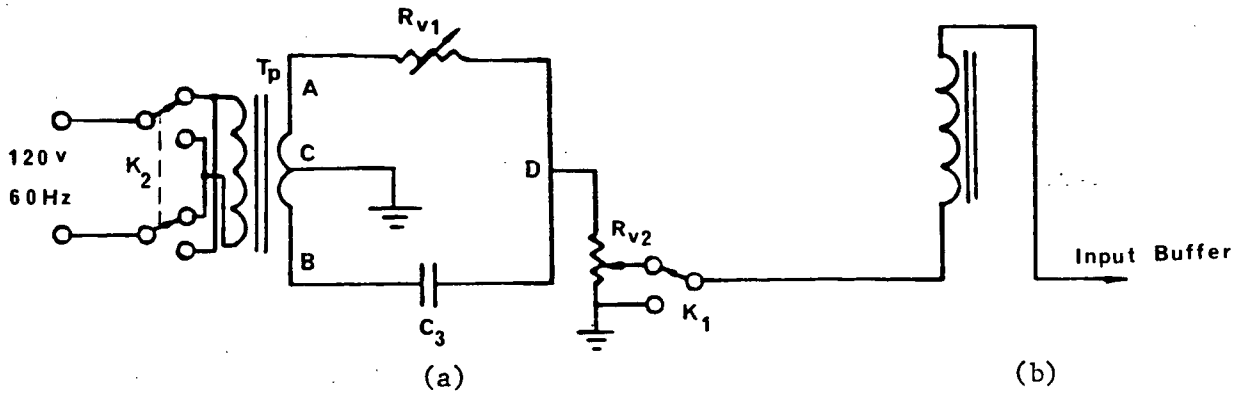


Fig 3.2 Circuit Components

(a) Phase Shifter

(b) Choke

(c) Phasor Diagram of Phase Shifter

(d) Input Buffer  $G_i$

(e) Attenuator  $G_a$

(f) Second Order Butterworth Low Pass Filter Stage (each of them from Filter 1 to Filter 6)

Table 3.1 Specification of Circuits in Fig 3.2

Choke	150 Henry		
Phase Shifter	$T_p$	120/6.3	$R_{v2}$ 0-500k $\Omega$
	$R_{v1}$	0-20 k $\Omega$	
	$C_3$	5 $\mu$ F	
Input Buffer	$R_{F1}$	100 k $\Omega$	
	$R_{f1}$	155 k $\Omega$	
	$R_p$	22 k $\Omega$	
Attenuator	$R_{a1}$	1 M $\Omega$	$G_{a1}=1$
	$R_{a2}$	150 k $\Omega$	$G_{a2} = \frac{R_{a2} + R_{a3}}{R_{a1} + R_{a2} + R_{a3}} = 1/7.4$
	$R_{a3}$	5.6 k $\Omega$	$G_{a3} = \frac{R_{a3}}{R_{a1} + R_{a2} + R_{a3}} = 1/206$
	$R_p$	22 k $\Omega$	
Filter1 to Filter6	$R_F$	50 k $\Omega$	
	$R_f$	10 k $\Omega$	
	$R_1$	6.8 k $\Omega$	
	$R_2$	56 k $\Omega$	
	C	0.32, 0.47, 1.0, 2.47, 4.4 $\mu$ F	

Note: Selection of  $R_F$ ,  $R_f$ ,  $R_1$ ,  $R_2$ , C for Filter1 to Filter6 is described in section 3.3

### 3.2 Inductive Device Choke

This device picks up, by magnetic induction, the signal frequency components of interest. The strength of the signal pickup depends upon the core size, inductance and the location of the choke relative to the motor. A choke with an inductance of 150 Henry is arbitrarily selected. The design of better transducer was not attempted.

### 3.3 Second Order Butterworth Low-Pass Filter

This is the most important part in the overall circuit and consists of six second order Butterworth filter stages. The second order low-pass Butterworth filter has flat characteristics in the pass band and rather sharp cut off in the stop band. No ripple in the frequency response curve makes the calculation of filter gain easier. The proper size of amplified slip frequency signal component after each stage of filtering should be obtained. The design of a second order Butterworth low-pass filter will be discussed in the following.

#### (1) Frequency Response Equation

The frequency response equation of each filter stage can be expressed as follows

$$G(\omega) = \frac{G}{1 - \left(\frac{\omega}{\omega_c}\right)^2 + 2\xi \left(j\frac{\omega}{\omega_c}\right)}$$

where  $G = 1 + \frac{R_F}{R_f}$  is the dc gain of the filter (3.3)

$$\omega_c = \sqrt{\frac{1}{R_1 R_2 C_1 C_2}} \quad \text{is the cut off frequency (3.4)}$$

$$\xi = \frac{1}{2} \left\{ \sqrt{\frac{R_2 C_2}{R_1 C_1}} + \sqrt{\frac{R_1 C_2}{R_2 C_1}} - (G-1) \sqrt{\frac{R_1 C_1}{R_2 C_2}} \right\} \quad (3.5)$$

is the damping coefficient

See the derivation in detail in Appendix A1.

When  $\xi = \frac{1}{\sqrt{2}}$  the filter equation is then

$$|G(\omega)| = \frac{G}{\sqrt{1 + \left(\frac{\omega}{\omega_c}\right)^4}} \quad (3.6)$$

and the  $\xi = \frac{1}{\sqrt{2}}$  substituting into eqn. (3.5)

$$\sqrt{\frac{R_2 C_2}{R_1 C_1}} + \sqrt{\frac{R_1 C_2}{R_2 C_1}} - (G - 1) \cdot \sqrt{\frac{R_1 C_1}{R_2 C_2}} = \sqrt{2} \quad (3.7)$$

The filter stage has an attenuation of -40 dB/decade and the total attenuation characteristic is proportional to the number of filter stages. The values of the circuit elements can be determined from the above three equations (3.3), (3.4), (3.7).

## (2) Parameter Value Determination

For simplicity of circuit calculation identical values were chosen for capacitors  $C_1$  and  $C_2$  in Figure 3.2 (f). Now eqn. (3.4), (3.7) become

$$f_c = \frac{1}{2\pi C} \sqrt{\frac{1}{R_1 R_2}} \quad (3.8)$$

where  $f_c$  is the corner frequency

$$\sqrt{\frac{R_2}{R_1}} + \sqrt{\frac{R_1}{R_2}} - (G - 1) \sqrt{\frac{R_1}{R_2}} = \sqrt{2} \quad (3.9)$$

From eqn. (3.8) the corner frequency  $f_c$  only depends upon the capacitor  $C$  if  $R_1$  and  $R_2$  are kept constant. Furthermore,  $R_1$  and  $R_2$  can be calculated from eqn. (3.3), (3.8), (3.9) once the parameters  $G$ ,  $f_c$  and  $C$  are given.

The values of  $f_c$ ,  $G$  and  $C$  are selected as follows:

a.  $f_c = 18 \text{ Hz}$

The corner frequency  $f_c$  is selected to be 18 Hz because it is basically sufficient for measurement of the whole range of motor since the overall

cut off frequency will decrease with an increasing number of filter stages. Most induction motors operate at speeds corresponding to slip  $s$  of less than 8% i.e.  $f_s$  less than 5 Hz.

$$b. G = 6 \quad \text{i.e. } G = 1 + \frac{R_F}{R_f} = 6$$

and  $R_F = 50 \text{ K } \Omega$ ,  $R_f = 10 \text{ K } \Omega$  are selected.

Considering the minimum slip frequency component  $V_s$  in choke voltage, which happens to be at the lowest slip frequency, a value of  $75 \times 10^{-6}$  was obtained (see Table 2.3) in the simple experiment of chapter 2. So this value of  $V_{s\min}$  should be amplified to the proper value  $V'_{s\min}$  after total six filter stages.

For the selection  $G = 6$ , the amplified output  $V'_{s\min}$  should be

$$V'_{s\min} = G^6 \cdot V_{s\min} = 6^6 \times 75 \times 10^{-6} = 3.5 \text{ volts}$$

Therefore, the output of 3.5 v at the sixth filter stage is a reasonable value to be measured and the selection  $G = 6$  is reasonable.

$$c. C = 0.47 \text{ } \mu\text{F}$$

By use of the above selecting parameter values, ( $G=6$ ,  $f_c=18 \text{ Hz}$ ,  $C=0.47 \times 10^{-6} \text{ F}$ ),  $R_1$  and  $R_2$  can be worked out by solving the eqn. (3.3), (3.8), (3.9) as follows:

$$G = 1 + \frac{R_F}{R_f} = 6$$

$$\text{since } f_c = \frac{1}{2\pi C} \cdot \sqrt{\frac{1}{R_1 R_2}}$$

$$R_1 R_2 = \frac{1}{(2\pi f_c C)^2} = \frac{1}{(2\pi \times 18 \times 0.47 \times 10^{-6})^2}$$

$$\text{so } R_1 R_2 = 0.0354 \times 10^{10} \quad (3.10)$$

$$\text{and } \sqrt{\frac{R_2}{R_1}} + \sqrt{\frac{R_1}{R_2}} - (6-1) \cdot \sqrt{\frac{R_1}{R_2}} = 1.414 \quad (3.11)$$

$$\text{Let } \chi = \sqrt{\frac{R_2}{R_1}}$$

substituting  $\chi$  into eqn. (3.11).

$$\chi + \frac{1}{\chi} - \frac{5}{\chi} = 1.414; \quad \chi^2 - 1.414\chi - 4 = 0$$

$$\chi = 2.83 \text{ or } -1.39$$

The correct solution is  $\chi = 2.83$

$$\text{Then } \sqrt{\frac{R_2}{R_1}} = 2.83 \quad R_2 = 8.0R_1$$

$$\begin{cases} R_2 = 8 R_1 \\ R_1 R_2 = 0.0354 \times 10^{10} \end{cases}$$

$$\begin{cases} R_1 = 6.65 \times 10^3 \Omega \\ R_2 = 53.5 \times 10^3 \Omega \end{cases}$$

Therefore,  $R_1 = 6.8 \text{ K } \Omega$  and  $R_2 = 56 \text{ K } \Omega$  using available resistor values.

Now verify the  $\xi$  and  $f_c$  by substituting the selected actual values  $R_1 = 6.8 \text{ K } \Omega$ ,  $R_2 = 56 \text{ K } \Omega$ ,  $C = 0.47 \mu\text{F}$  into eqn. (3.5), (3.8).

$$\begin{aligned} \text{so } \xi &= \frac{1}{2} \left\{ \sqrt{\frac{R_2}{R_1}} + \sqrt{\frac{R_1}{R_2}} - (6-1) \cdot \sqrt{\frac{R_1}{R_2}} \right\} \\ &= 0.5 \left\{ \sqrt{\frac{56}{6.8}} + \sqrt{\frac{6.8}{56}} - (6-1) \cdot \sqrt{\frac{6.8}{56}} \right\} \\ &= 0.74 \end{aligned}$$

$$\begin{aligned} f_c &= \frac{1}{2\pi C} \cdot \frac{1}{\sqrt{R_1 R_2}} = \frac{1}{6.28 \times 0.47 \times 10^{-6}} \sqrt{\frac{1}{6.8 \times 56 \times 10^6}} \\ &= 17.3 \text{ Hz} \end{aligned}$$

The actual  $\xi = 0.74$  and  $f_c = 17.3$  Hz are close to the selected values of  $f_c = 18$  Hz and  $\xi = 0.707$ . The corner frequency  $f_c$  is varied by using different values of capacitors while keeping all other element values fixed.

$$C = 0.32, 0.47, 1.0, 2.47, 4.4 \mu\text{F}$$

The attenuation for each filter stage is -40 dB/decade and the total attenuation from input to output is proportional to the number of stages employed. Successful detection of slip frequency for measuring each speed heavily rely upon the reasonable selection of both corner frequency and total attenuation.

#### 3.4 Input Buffer and Attenuator

The input stage of the measuring circuit consists of a noninverting operational amplifier with high input impedance, as indicated in Figure 3.1, Figure 3.2(d). If the signal from the choke, which has high inductance, is directly connected to the first filtering stage that includes the capacitance feedback circuit the circuit will become unstable and oscillations will take place. Therefore, the input operational amplifier acts as a buffer stage between the choke signal source and the input of the first filter stage.

As mentioned previously, the design of each filter stage must be such that the weak slip frequency signal component  $V_s$  will be amplified and the supply frequency signal component will be attenuated. The ratio of these two signals  $V_{60}$  to  $V_s$  at any filter stage indicates the degree of filtering. Where more than four stages of filtering is required, the attenuator circuit is required to maintain operation in the linear region of the operational amplifier. Alternatively, attenuation could have been provided in each filter stage.

### 3.5 Phase Shifter

One of the objectives to use a filter is to attenuate the supply frequency signal component 60 Hz in the mixed source signal so that the slip frequency component can be identified, thus the ratio of  $V_{60}$  to  $V_s$  can be minimized after each filter stage. The phase shifter having supply frequency can also be used in the same role as the filter by providing a phase-shafted supply frequency signal. How it works is shown in Figures 3.1, 3.2. The phase shifter (Figure 3.1) can vary its output phase relative to the phase of the supply frequency component of the choke voltage. Let the phase shifter output superpose on the choke voltage and adjust the phase and magnetude of phase shifter output. Then the input of buffer will have a greatly attenuated supply frequency component. Hence the number of filter stages required would be less. The major components in the phase shifter shown in Figure 3.2(a) include the centre-tapped transformer  $T_p$ , variable resistor  $R_{v1}$  and capacitor  $C_3$ . The function of  $T_p$  is to reduce the supply voltage to a suitable size.

The principle of phase shifter can be readily found in the circuit diagram Figure 3.2(a),(c). The fixed supply voltage  $V_{AB}$  with centre tap supplies the series RC circuit in the closed-loop circuit ACBD. The voltage  $V_{DB}$  across  $C_3$  always lags by  $90^\circ$   $V_{AD}$  across the variable resistor  $R_{v1}$ . The potential D relative to ground C will move on the circle shown in Figure 3.2(c) if the resistor  $R_{v1}$  varies. In order to obtain a variable voltage output  $R_{v2}$  is used. The switch  $K_2$  is a reversing switch which allows the phase shifter to work in another half circle. For example, once the  $K_2$  reverses, the potential D will fall into symmetric  $D'$  in the next half circle (Figure 3.2(c)). So the range of phase angle for this circuit can change theoretically from  $0^\circ$  to  $360^\circ$ . However, it

is impossible to use an infinite value of capacitor, and the actual range of phase shifter mainly depends upon the size of capacitor used.

## 4. EXPERIMENTAL RESULTS

The proposed method of speed measurement was tested on four different induction motors. The specifications for these motors are given in Table 4.1.

Table 4.1 Motor Specifications

Motor	Full Load Speed (rpm)	Type of Motor	Horse Power P (Hp)	Rated Current I (a)	Rated Voltage V (v)
M1	1725	3-phase wound rotor	1/3	1.7	220
M2	1725	3-phase squirrel cage	1/4	1.5	220
M3	1725	1-phase squirrel cage	1/4	5.5	120
M4	1690	3-phase wound rotor	2.5	8	208

The experimental setup is shown in Figure 4.1. A choke is placed in the vicinity of the test motor and is left in position throughout the test. Its output is taken to a filter, as discussed in chapter 3. The filter output is then fed to a Universal Waveform Analyzer which is a 68000 micro-processor-based instrument. The dc generator is mechanically-coupled to the induction motor, and with its resistance load provides a variable motor load. The actual motor speed is measured by a stroboscope for comparison with that determined from the slip frequency. The number of filter stages, value of filter capacitor and attenuator gain were adjusted for best slip frequency determination. The amplitude of the slip frequency signal component can be determined by the use of the filter gain formulae and characteristic curves as described in appendix A2.

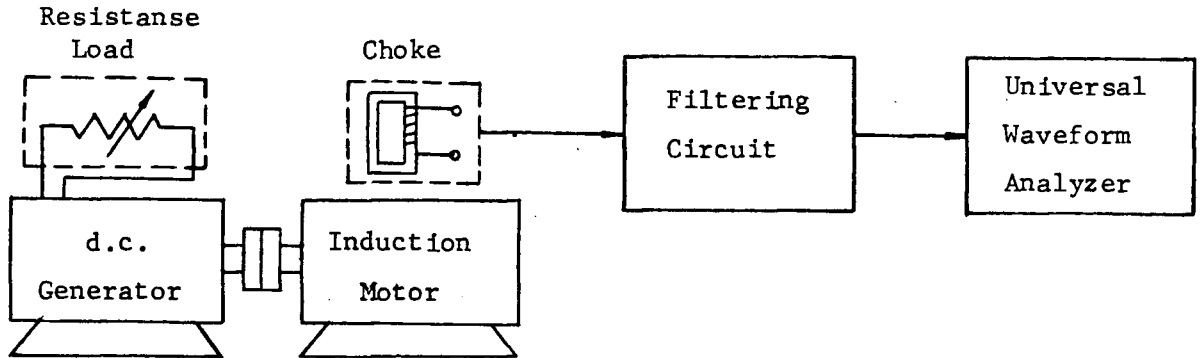


Fig 4.1 Experimental Setup

Experimental results for the four induction motors are given in Table 4.2 to 4.5. The following symbols are used in the Tables.

$I$	Motor current
$n_a$	Actual speed measured by the stroboscope, (* means speed at or closest to rated speed )
$N$	Number of the filter stages at which the output is measured
$C$	Value of capacitor used in the filter stages
$G_a$	Gain of the attenuator
$f_s$	Slip frequency
$v_s$	Amplitude of $f_s$ at the filter output
$f_n$	Frequency of "noise" signal
$v_n$	Amplitude of $f_n$ at filter circuit output
$n_1$	Motor speed calculated from the measured $f_s$ through (1.7)
$v_{sin}$	Calculated input amplitude of the $f_s$ component by eqn. (A2.14)
$v_{nin}$	Calculated input amplitude of the $f_n$ component by eqn. (A2.14)
$v_{60}$	Induced supply frequency (60 Hz) amplitude in the choke

Table 4.2 Experimental Results of Motor M1

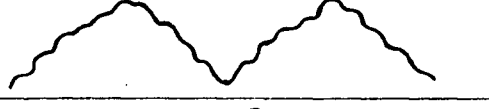
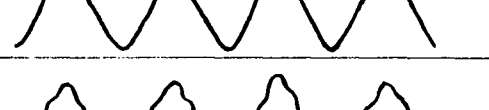
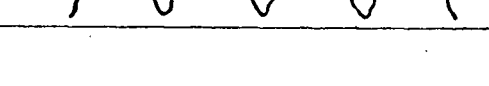
Motor		Filtering Circuit			Output of Filtering Circuit						Input		$V_{60}/V_{sin}$ ( $\times 10^3$ )
I (a)	$n_a$ (rpm)	N	C ( $\mu F$ )	$G_a$	Waveform	$f_s$ (Hz)	$V_s$ (v)	$f_n$ (Hz)	$V_n$ (v)	Calculated		$V_{60}$ (v)	
										$n_1$ (rpm)	$V_{sin}$ (mv) $V_{nin}$		
1.14	1770	3	1.0			0.98	0.24	2.93	.032	1770	0.73 0.1	1.02	1.4
		6	0.32	1/206			0.18	30	0.14		0.52 8.3		
1.2	1755	3	1.0			1.56	0.44	4.3	.034	1753	1.41 0.12	1.07	0.76
		6	0.32	1/206				30	0.16		9.5		
1.3	1740	3	1.0			1.94	0.74			1742	2.25	1.1	0.49
		6	0.32	1/206			0.65	30	0.18		1.87 10.7		
1.45	1710*	3	1.0			2.96	0.12			1711	3.8	1.18	0.3
		6	0.32	1/206			1.13	30	0.23		3.3 13.6		
1.65	1680	3	1.0			3.9	1.86			1683	6.5	1.29	0.20
		6	0.32	1/206			1.67	30	0.3		4.96 17.8		

Table 4.2 (continued)

Motor		Filtering Circuit			Output of Filtering Circuit						Input		$V_{60}/V_{sin}$ ( $\times 10^3$ )
I (a)	$n_a$ (rpm)	N	C ( $\mu F$ )	$G_a$	Waveform	$f_s$ (Hz)	$V_s$ (v)	$f_n$ (Hz)	$V_n$ (v)	Calculated		$V_{60}$ (v)	
										$n_1$ (rpm)	$V_{sin}$ (mv)		
1.86	1650	3	1.0			5.08	2.16			1647	8.49	1.33	0.16
		6	0.32	1/206			2.23	30	0.31		6.7 18.4		
2.06	1620	3	1.0			5.86	2.03			1624	9.89	1.37	0.14
		6	0.32	1/206			2.75	30	0.33		8.4 19.6		

† : In these two cases each one has a low rate of oscillation 2.93 Hz & 4.3 Hz about its centre speed 1770 & 1755 as observed by a stroboscope

Table 4.3 Experimental Results of Motor M2

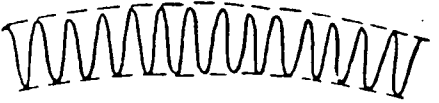
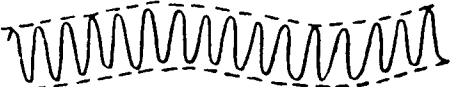
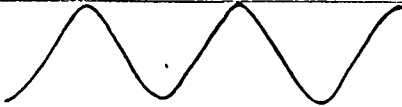
Motor		Filtering Circuit			Output of Filtering Circuit						Input		$V_{60}/V_{sin}$ ( $\times 10^3$ )
I (a)	$n_a$ (rpm)	N	C ( $\mu F$ )	$G_a$	Waveform	$f_s$ (Hz)	$V_s$ (v)	$f_n$ (Hz)	$V_n$ (v)	Calculated		$V_{60}$ (v)	
										$n_1$ (rpm)	$V_{sin}$ (mv) $V_{nin}$		
1.1	1778	3	4.4			0.73	.052			1778	0.186	0.38	2.04
		6	0.32	1/7.4				30	19.1		40.8		
1.1	1767	3	4.4			1.1	.067			1767	0.27	0.362	1.15
		6	0.32	1/7.4				30	17.5		37.4		
1.15	1755	3	4.4			1.52	.055			1754	0.34	0.345	1.01
		6	0.32	1/7.4				30	15.2		32.5		
1.15	1740	3	4.4			1.96	.034			1741	0.46	0.346	0.75
		6	0.32	1/7.4				30	13.5		28.9		
1.15	1725*	5	1.0			2.5	.74			1725	0.50	0.362	0.72
		6	0.32	1/7.4				30	9.51		20.4		

Table 4.3 (continued)

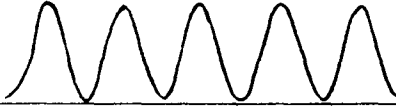
Motor		Filtering Circuit			Output of Filtering Circuit						Input		$V_{60}/V_{sin}$ ( $\times 10^3$ )
I (a)	$n_a$ (rpm)	N	C ( $\mu F$ )	$G_a$	Waveform	$f_s$ (Hz)	$V_s$ (v)	$f_n$ (Hz)	$V_n$ (v)	Calculated		$V_{60}$ (v)	
										$n_1$ (rpm)	$V_{sin}$ (mv) $V_{nin}$		
1.2	1710	5	1.0	1/7.4		2.92	.792			1712	0.552	0.346	0.63
		6	0.32	1/7.4				30	8.14		17.4		
1.27	1695	5	1.0	1/7.4		3.46	.865			1696	0.646	0.337	0.52
		6	0.32	1/7.4				30	7.14		15.2		
1.37	1680	5	1.0	1/7.4		4.1	.933			1677	0.728	0.334	0.46
		6	0.32	1/7.4				30	6.28		13.4		

Table 4.4 Experimental Results of Motor M3

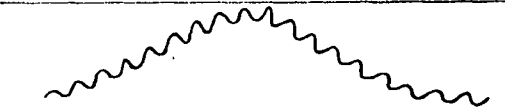
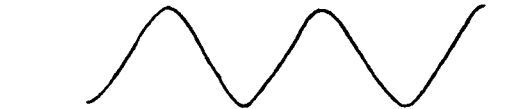
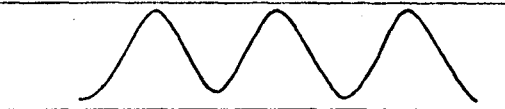
Motor		Filtering Circuit			Output of Filtering Circuit						Input		$V_{60}/V_{sin}$ ( $\times 10^3$ )
I (a)	$n_a$ (rpm)	N	C ( $\mu F$ )	$G_a$	Waveform	$f_s$ (Hz)	$V_s$ (v)	$f_n$ (Hz)	$V_n$ (v)	Calculated		$V_{60}$ (v)	
										$n_1$ (rpm)	$V_{sin}$ (mv) $V_{nin}$		
5.1	1882	5	1.0	1/7.4		0.61	0.31			1782	0.21	3.88	18.5
		6	0.32	1/7.4				30	4.5		9.6		
5.1	1770	5	1.0	1/7.4		1.03	.547			1769	0.37	3.44	9.3
		6	0.32	1/7.4				30	3.7		7.9		
5.16	1755	5	1.0	1/7.4		1.48	.801			1756	0.56	3.11	5.5
		6	0.32	1/7.4				30	3.2		6.8		
5.4	1740	5	1.0	1/7.4		2.07	.946			1738	0.68	2.96	4.4
		6	0.32	1/7.4				30	2.5		5.3		
5.7	1725*	5	1.0	1/7.4		2.53	1.0			1724	0.73	2.7	3.7
		6	0.32	1/7.4				30	2.1		4.5		

Table 4.4 (continued)

Motor		Filtering Circuit			Output of Filtering Circuit						Input		$V_{60}/V_{sin}$ ( $\times 10^3$ )
I (a)	$n_a$ (rpm)	N	C ( $\mu F$ )	$G_a$	Waveform	$f_s$ (Hz)	$V_s$ (v)	$f_n$ (Hz)	$V_n$ (v)	Calculated		$V_{60}$ (v)	
										$n_1$ (rpm)	$V_{sin}$ (mv)		
5.95	1710	5	1.0	1/7.4		2.94	1.09			1712	0.814	2.48	3.0
		6	0.32	1/7.4				30	1.8		3.9		

Table 4.5 Experimental Results of Motor M4

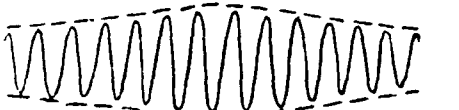
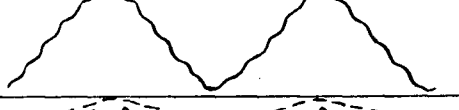
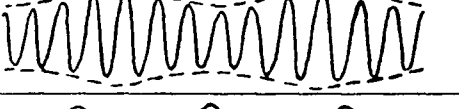
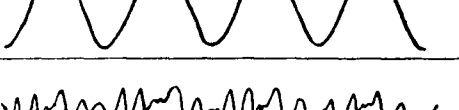
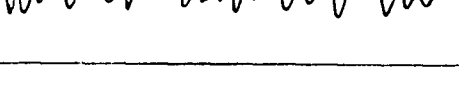
Motor		Filtering Circuit			Output of Filtering Circuit						Input		$V_{60}/V_{in}$ ( $\times 10^3$ )
I (a)	$n_a$ (rpm)	N	C ( $\mu F$ )	$G_a$	Waveform	$f_s$ (Hz)	$V_s$ (v)	$f_n$ (Hz)	$V_n$ (v)	Calculated		$V_{60}$ (v)	
										$n_1$ (rpm)	(mv) $V_{sin}$ $V_{n/in}$		
1.3	1770	3	4.4			1.05	.029			1769	0.11	0.45	3.5
		3	1.0			1.04	.034			1769	0.128		
		6	0.32	1/7.4				30	5.55		15.9		
1.72	1740	3	4.4			2.03	.017			1739	0.23	0.48	2.0
		3	1.0			2.05	.079			1739	0.24		
		6	0.32	1/7.4				30	13.8		29.5		
2.2	1710	3	1.0			3.08	0.11			1708	0.35	0.50	1.45
		6	0.32	1/7.4				30	15.7		33.6		
2.7	1680*	3	1.0			3.9	0.17			1683	0.58	0.50	0.87
		6	0.32	1/7.4				15.6	1.74		0.28		
								24.4	6.9		4.9		

Table 4.5 (continued 1)

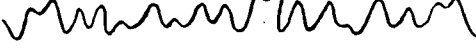
Motor		Filtering Circuit			Output of Filtering Circuit						Input		$V_{60}/V_{sin}$ ( $\times 10^3$ )
I (a)	$n_a$ (rpm)	N	C ( $\mu F$ )	$G_a$	Waveform	$f_s$ (Hz)	$V_s$ (v)	$f_n$ (Hz)	$V_n$ (v)	Calculated		$V_{60}$ (v)	
										$n_1$ (rpm)	$V_{sin}$ (mv)		
3.23	1650	3	1.0			5.1	0.2			1647	0.79	0.50	0.63
		6	0.32	1/7.4				12.7	2.0		0.27		
3.7	1620	3	1.0			6.04	0.23			1617	1.1	0.50	0.45
		6	0.32	1/7.4				21	12.5		4.04		
4.22	1590	3	1.0			7.01	0.24			1586	1.55	0.51	0.33
		6	0.32	1/206				19.5	0.66		4.8		
4.57	1560	3	1.0			8.0	0.23			1560	2.02	0.51	0.25
		6	0.32	1/206				12.7	0.37		1.35		
4.9	1530	3	1.0			9.1	0.16	6.84	0.12	1527	2.03	0.51	0.25
		6	0.32	1/206				16.6	.015		0.74 .075		

Table 4.5 (continued 2)

Motor		Filtering Circuit			Output of Filtering Circuit						Input		$V_{60}/V_{sin}$ ( $\times 10^3$ )	
I (a)	$n_a$ (rpm)	N	C ( $\mu F$ )	$G_a$	Waveform	$f_s$ (Hz)	$V_s$ (v)	$f_n$ (Hz)	$V_n$ (v)	Calculated				$V_{60}$ (v)
										$n_1$ (rpm)	$V_{sin}$ (mv)	$V_{nin}$		
5.3	1500	3	1.0			10.0	0.13	4.9	.031	1500	2.4	0.12	0.52	0.25
		6	0.32	1/206				14.7	.024					
5.7	1440	3	1.0			12.1	.068			1440	3.3	0.52	0.16	
		6	0.32	1/206				0.91	1.06					
5.9	1380	6	0.32	1/206		13.7	0.67	8.8	0.87	1369	4.5	0.53	0.12	
6.4	1320	6	0.32	1/206		15.9	1.16	5.86	0.57	1323	5.3	0.55	0.10	
6.8	1260	6	0.32	1/206		18.1	1.24	2.73	0.32	1257	7.16	0.56	.078	
7.5	1200	6	0.32	1/206		20.0	1.0	1.95	0.17	1200	7.7	0.58	.076	

#### 4.1 Discussion of Experimental Results

The basic idea of using the slip frequency to determine the speed of induction motors relies on counting the zero axis crossings of the output signal waveform from the filter. Therefore, the shape of the waveform is important. Any distortion in the signal waveform will affect the speed measurement. The signal waveform can be classified as follows:

(1) There is no distortion and the signal frequency is exactly equal to the slip frequency  $f_s$ .

(2) The waveform contains some noise but the frequency of the waveform is still equal to the slip frequency  $f_s$ .

(3) There is considerable distortion in the waveform so that the frequency of the waveform is no longer equal to the slip frequency  $f_s$ .

The results for all measured filter outputs according to the above waveform classification are listed in Table 4.6. The expected and measured slip frequency for each motor speed are shown in Figure 4.2. From Figure 4.2 and Table 4.6 some important points can be deduced as follows:

(1) The speed of an induction motor within the rated load, i.e. for  $s < 13\%$ , or  $f_s < 8$  Hz, can be accurately measured by the proposed method.

(2) The measured slip frequency would be fully equal to the expected value if there are no unstable factors, such as fluctuations in the motor speed.

(3) Proper filter parameter values, such as the corner frequency  $f_c$ , must be chosen to eliminate any noise in the output signal. The selection of  $C = 1.0 \mu F$ , i.e.,  $f_c = 4.5$  Hz for three stages appears to be suitable for the four test motors used.

Table 4.6 Waveform Evaluation of Detected Slip Frequency

Motor	C ( $\mu$ F)	n (rpm)	1770	1755	1740	1725	1710	1695	1680	1650	1620
		$f_s$ (Hz)	1	1.5	2	2.5	3	3.5	4	5	6
M1	1.0		o	o	o		o		o	o	o
	0.32		$\Delta$	$\Delta$	$\Delta$		$\Delta$		$\Delta$	$\Delta$	$\Delta$
M2	4.4 or 1.0		o	o	o	o	o	o	o		
	0.32		x	x	x	x	x	x	x		
M3	1.0		o	o	o	o	o				
	0.32		$\Delta$	$\Delta$	$\Delta$	$\Delta$	$\Delta$				
M4	4.4		o		o						
	1.0		$\Delta$		$\Delta$		o		o	o	o
	0.32		x		x		x		x		

Motor	C ( $\mu$ F)	n (rpm)	1590	1560	1530	1500	1440	1380	1320	1260	1200
		$f_s$ (Hz)	7	8	9	10	12	14	16	18	20
M4	1.0		o	o	x	$\Delta$	$\Delta$				
	0.32		x	x	x	x	$\Delta$	x	$\Delta$	o	$\Delta$

Case (1) : o

Case (2) :  $\Delta$

Case (3) : x

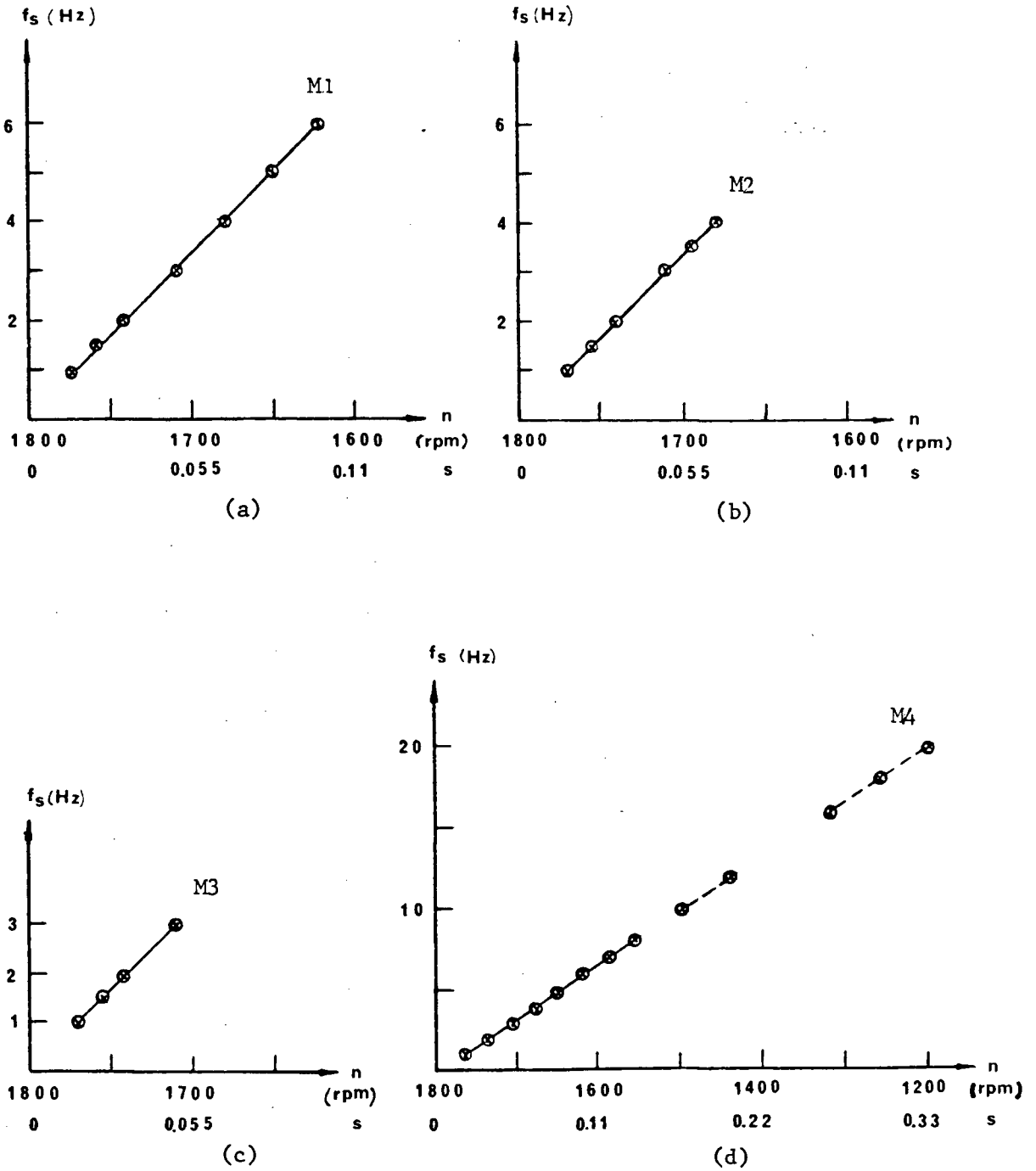


Fig 4.2 Comparison of Expected and Detected Slip Frequency for Induction Motor (a) M1 (b) M2 (c) M3 (d) M4  
 × expected value      o detected value  
 — case (1)      - - - case (2)

#### 4.2 Supply Frequency Signal Component

The amplitude of the supply frequency  $f_{60}$  (60 Hz) component that is induced in the choke, of course, depends upon the location of the choke with respect to the motor. Usually the choke is placed as close as possible to the motor so as to pick up a strong signal. The 60 Hz signal is the most important signal to be filtered out in the process of detecting the slip frequency. The number of filter stages required not only depends upon the amplitude of the 60 Hz signal but more importantly upon the amplitude ratio of the 60 Hz signal to the  $f_s$  signal. The  $v_{60}/v_f$  ratios of four motors are measured and indicated in Figure 4.3.

It is found that the amplitude of the slip frequency signal increases greatly with increasing slip whereas the amplitude of the supply frequency signal varies very slightly. From experimental results the slip frequency amplitude  $v_{sin}$  can be considered to be approximately proportional to the product of the motor current and the slip frequency.

$$v_{sin} \propto I \cdot f_s \quad (4.1)$$

The ratio of the amplitude of the supply frequency signal to the amplitude of the slip frequency signal governs how many filter stages are required. However, the closer the slip frequency is to the supply frequency, the more difficult is the filtering.

#### 4.3 Measurement of Pole Pairs

The motor speed  $n_1$  not only depends upon the measured slip frequency  $f_s$  but is also related to the pole pairs,  $p$ , as given in equation (1.6) and rewritten below:

$$n_1 = \frac{f - f_s}{p} 60 \quad (1.6)$$

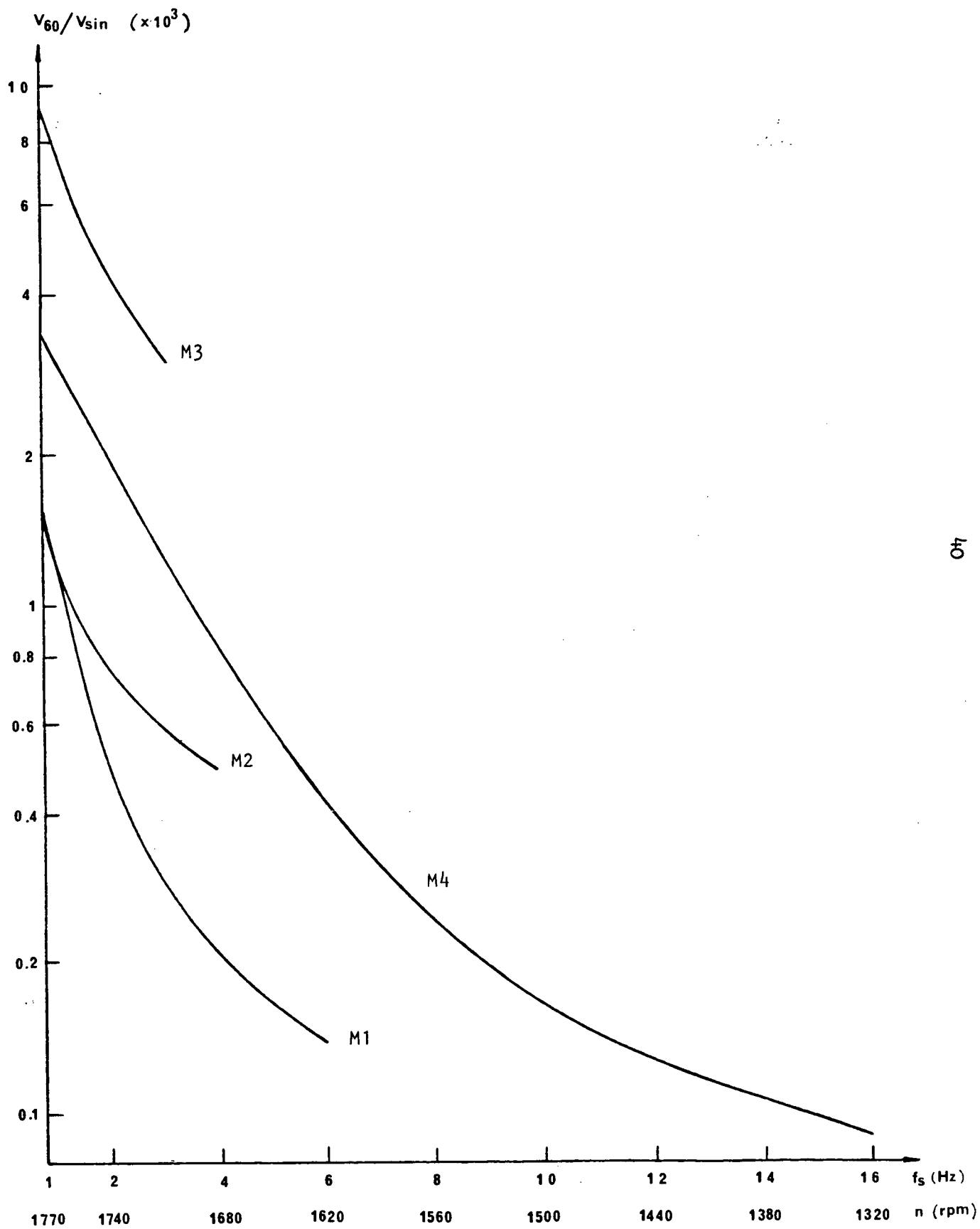


Fig 4.3 Amplitude Ratio of 60 Hz Supply Frequency Signal to Slip Frequency Signal

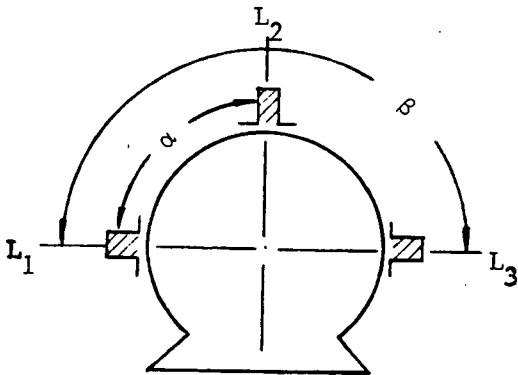


Fig 4.4 Location Diagram  
of Pole Pair  
Measurement

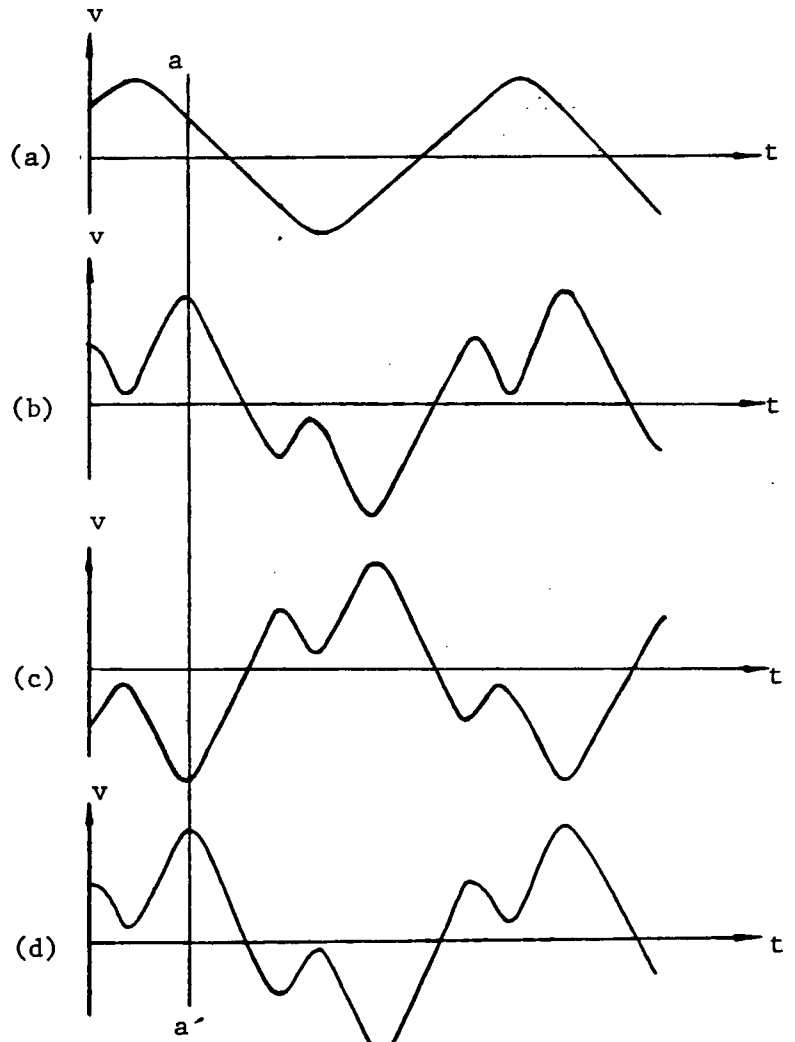


Fig 4.5 Choke Voltage Waveform at  
Several Locations

(a) Supply Frequency Reference  
Waveform

(b) at  $L_1$  (c) at  $L_2$  (d)  $L_3$

The following experiment illustrates one way to measure the pole-pair value. The experiment uses the induction motor M3, which is single phase. With the motor running, the position of the choke is varied around the

motor surface, as indicated in Figure 4.4. The choke voltage is connected to one channel of a two-channel oscilloscope while the 60 Hz supply waveform is connected to the other channel and is used as timing reference (shown in Figure 4.5(a)). The waveform of the choke voltage for different location  $L_1$ ,  $L_2$  and  $L_3$  (here  $\alpha=90^\circ$ ,  $\beta=180^\circ$ ) are shown in Figure 4.5(b), (c),(d), respectively. With the choke at location  $L_1$  the leftmost peak value of the choke voltage is noted to be on the assumed vertical line  $aa'$  indicates that the mechanical angle  $\alpha$  is electrically equivalent to  $180^\circ$ . Similarly, moving the choke to location  $L_3$  will place the peak value back at line  $aa'$  so that the mechanical angle  $\beta$  is electrically  $360^\circ$ . Therefore, the pole-pair value of the motor can be obtained as follows:

$$p = \frac{360^\circ}{2\alpha} \quad (4.2)$$

$$p = \frac{360^\circ}{\beta} \quad (4.3)$$

In this example  $\alpha=90^\circ$   $\beta=180^\circ$

so  $p=2$ .

It is not very hard to explain. The choke voltage waveform at each location with respect to the motor usually are the same but its phase angle with respect to the supply voltage varies. Therefore, the relation between electrical and mechanical angle will yield the pole-pair value as given by equations (4.2) and (4.3).

## 5. CONCLUSION

A method of measuring the motor speed of an induction motor by detection of the slip frequency signal has been proposed in this thesis. The measurement can be made without attachment of any devices to the motor shaft. In fact, the motor may be completely enclosed so that conventional speed measurement by the use of tachometers or stroboscopes would not be possible.

Experimental results indicate good agreement between actual motor speed and that measured by the proposed slip frequency method in the range below a slip frequency of about 8 Hz that is within the range of most 60 Hz induction motors. The method is suitable for both single- and three-phase induction motors and will be applicable to sealed motors, such as motors used in refrigerators, since access to the motor shaft is not needed.

The proposed method does require knowledge of the number of poles in the motor. A simple method to determine this experimentally was discussed in chapter 4.

The speed measurement circuit described in chapter 3 needs to be improved in the following respects:

- (1) The inductive transducer should be optimized for best slip-frequency signal pickup.
- (2) Instead of detection by the waveform analyzer the slip frequency signal or the corresponding motor speed signal should be made available for display or for use in any speed control loop.
- (3) The filtering and amplifying stages could be optimized for sharper cut-off and improved signal-to-noise ratio of the desired slip frequency signal.

## REFERENCES

1. Sawaki, N. and Sato, N., "Steady-State and Stability Analysis of Induction Motor Driven by Current Source Inverter", IEEE Trans. on IA. Vol. IA-13, pp.244-253. May/June, 1977.
2. Plunkett, A.B., "Direct Flux and Torque Regulation in a PWM Inverter-Induction Motor Drive", IEEE Trans. on IA, Vol. IA-13, pp.139-146, Mar./Apr., 1977.
3. Plunkett, A.B., D'Atre, J.D. and Lipo, T.A., "Synchronous Control of a Static AC Induction Motor Drive", IEEE Trans. on IA, Vol. IA-15, pp.430-437, Jul./Aug., 1979.
4. Nabace, A., Otsuka, K., Uchino, H. and Kurosawa, R., "An Approach to Flux Control of Induction Motors Operated with Variable-Frequency Power Supply", IEEE Trans. on IA, Vol. IA-16, pp.342-350, May/June, 1980.
5. Bouler, P. and McLarren, S.G., "Slip-Frequency Limited Phase-Locked Loop Induction-Motor Drive", IEE Proc., Vol. 127, pt.d, pp.51-54, Mar. 1980.
6. Moore, A.W., "Phase-Locked Loop for Motor Speed Control", IEEE Spectrum, 1973, April (10), pp.61-67.
7. Ishida, M. and Iwata, K., "A New Slip Frequency Detector of an Induction Motor Utilizing Rotor Slot Harmonics", IEEE/IAS, 1982 ISPC Conf. Rec., pp.408-415.
8. Ishida, M. and Iwata, K., "A Slip Frequency Detection Method of Induction Motor Utilizing Rotor Slot Harmonics", Conf. Rec. of 1980 Tokai Region Annual Meeting of IEE of Japan, pp.153, Nov. 1980.

9. Maisel, J.E. and Klingshirn, E.A., "Low-Frequency Spectral Analysis Using a Dynamometer-Type Wattmeter", IEEE Trans. on Education, Vol. E-25, No. 2, May 1982.
10. Davold, W., Circuit Design for Electronic Instrumentation.

## APPENDICES

Al. Derivation of the Frequency Response Equation for Second Order Butterworth Low-Pass Filter

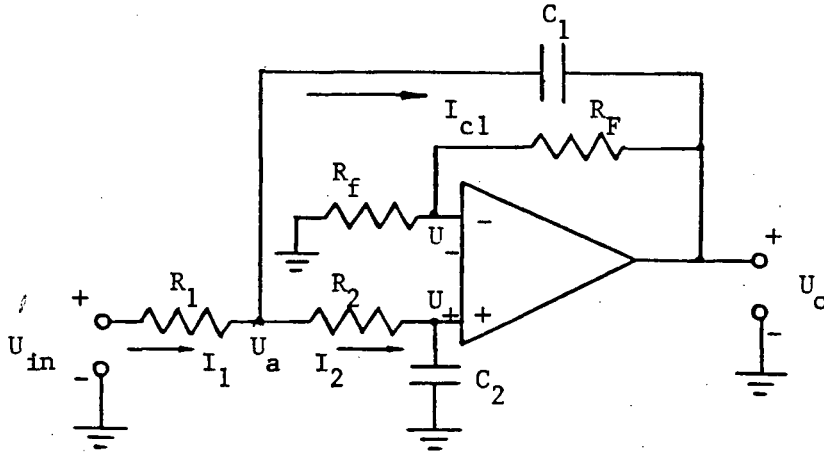


Fig Al.1 Second Order Butterworth Low-Pass Filter

The noninverting second order low pass filter shown in Figure Al.1 is used for the derivation. The derivation is based upon the "Virtual Ground Analysis" and assumes that

- (1) The open-loop gain of the operational amplifier is infinite, i.e.,  $G_o = \infty$
- (2) Input impedance is infinite  $Z_i = \infty$ . Therefore, input current  $I_n = 0$ .
- (3) Input voltage  $u_+ - u_- = 0$

Equations for Figure Al.1 by normal circuit analysis are as follows:

$$u_- = \frac{R_f}{R_f + R_F} u_o \quad (\text{Al.1})$$

$$u_+ = \frac{1}{1 + j\omega R_2 C_2} u_a \quad (\text{Al.2})$$

$$I_1 = \frac{1}{R_1}(u_{in} - u_a) \quad (A1.3)$$

$$I_{c1} = j\omega c_1(u_a - u_o) \quad (A1.4)$$

$$I_2 = \frac{1}{R_2}(u_a - u_+) \quad (A1.5)$$

$$I_1 = I_2 + I_{c1} \quad (A1.6)$$

Solving this group of equations the gain of filter  $G(\omega)$  is expressed as

$$G(j\omega) = \frac{u_o}{u_{in}} = \frac{G}{(j\frac{\omega}{\omega_c})^2 + 2\xi(j\frac{\omega}{\omega_c}) + 1}$$

$$G(\omega) = \frac{G}{1 - (\frac{\omega}{\omega_c})^2 + 2\xi(j\frac{\omega}{\omega_c})} \quad (A1.7)$$

where  $\xi$  is the damping coefficient

$\omega_c$  is the inherent angular corner frequency

Therefore, the amplitude response  $G(\omega)$  and phase response  $\phi(\omega)$  is readily obtained by equation (A1.7).

$$G(\omega) = \frac{G}{\sqrt{\left(1 - \frac{\omega^2}{\omega_c^2}\right)^2 + \left(2\xi \frac{\omega}{\omega_c}\right)^2}} \quad (A1.8)$$

$$\phi(\omega) = -\tan^{-1} \frac{2\xi \frac{\omega}{\omega_c}}{1 - \left(\frac{\omega}{\omega_c}\right)^2} \quad (A1.9)$$

where 
$$G = 1 + \frac{R_F}{R_f} \quad (A1.10)$$

$$\omega_c = \sqrt{\frac{1}{R_1 R_2 C_1 C_2}} \quad (A1.11)$$

$$\xi = \frac{1}{2} \left\{ \sqrt{\frac{R_2 C_2}{R_1 C_1}} + \sqrt{\frac{R_1 C_2}{R_2 C_1}} - (G-1) \sqrt{\frac{R_1 C_1}{R_2 C_2}} \right\} \quad (A1.12)$$

when  $\xi = \frac{1}{\sqrt{2}}$

equation (A1.8) becomes

$$G(\omega) = \frac{G}{\sqrt{1 + \left(\frac{\omega}{\omega_c}\right)^4}} \quad (A1.13)$$

This is the second order Butterworth filter response.

Substituting  $\xi = \frac{1}{\sqrt{2}}$  into eqn. (A1.12)

we therefore require

$$\sqrt{\frac{R_2 C_2}{R_1 C_1}} + \sqrt{\frac{R_1 C_2}{R_2 C_1}} - (G-1) \sqrt{\frac{R_1 C_1}{R_2 C_2}} = \sqrt{2} \quad (A1.14)$$

## A2. Calculation of Slip Frequency Signal Component

### A2.1 Gain Formulae and Curves of Three Filter Stages in Cascade

The gain of three identical filter stages in cascade, as indicated in Figure 3.1 is given by:

$$\frac{V_{3out}}{V_{in}} = G_i \cdot G_f^3 \quad (A2.1)$$

where  $V_{3out}$  is the output of the third filter stage

$V_{in}$  is the input to the input buffer

$G_i$  is the gain of input buffer

$G_f$  is the gain of a single filter stage

Usually the gain is expressed in decibels, which is defined as follows:

$$G_{3db} = 20 \log_{10} \frac{V_{3out}}{V_{in}} \bigg/ \frac{V_{3oout}}{V_{oin}} \quad (A2.2)$$

where  $V_{3oout}$  is the output of the third filter stage at  $f = 0$

$V_{oin}$  is the input  $V_{in}$  at  $f = 0$

$G_{3db}$  is the total gain in dB, the input buffer and the three filter stages in cascade

The gain curves in Figure A2.1 are plotted from measurements made for three filter stages in cascade for various values of capacitors  $C$ . These curves will be used as calculation of measured slip frequency amplitude for various induction motor speeds.

### A2.2 Calculation of Slip-Frequency Signal Amplitude Through Any Number of Filter Stages

The number of filter stages actually used in slip frequency measurements differ for various induction motors. The calculation of slip-frequency signal amplitude will be discussed here. In Figure 3.1 the attenuator,  $G_a$ ,

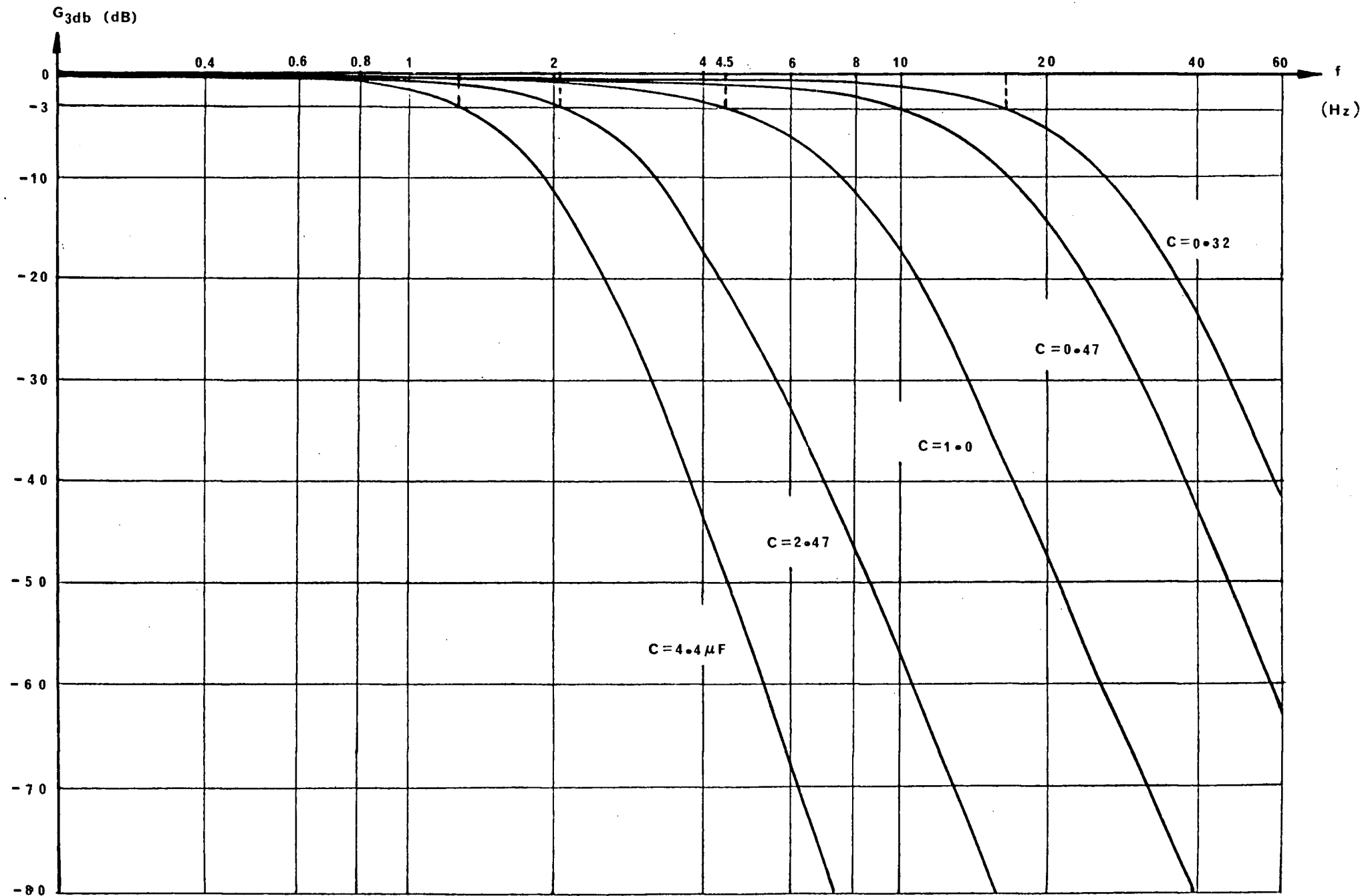


Fig A2.1 Gain Curves of three Identical Second Order Butterworth Filter Stages in Cascade

is inserted between the third and the fourth filter stage, so that the derivation of the gain equation will be divided into two cases as follows:

(1) When  $N \leq 3$

Where  $N$  is the number of filter stages. The gain for  $N$  filter stages is given by

$$G_N = \frac{V_{Nout}}{V_{in}} \quad (A2.3)$$

Where  $V_{Nout}$  is the output of the  $N$ th filter stage.

From Figure 3.1

$$G_N = (G_f)^N G_i \quad (A2.4)$$

Assume

$$G_{No} = \frac{V_{Noout}}{V_{oin}} \quad (A2.5)$$

Where  $G_{No}$  is the gain  $G_N$  at  $f = 0$

$V_{Noout}$  is the output  $V_{Nout}$  at  $f = 0$

So

$$G_{No} = (G_{fo})^N G_{io} = (G_{fo})^N G_i \quad (A2.6)$$

Where  $G_{fo}$  is the gain  $G_f$  at  $f = 0$

and  $G_i = G_{io}$

Therefore, the gain in dB is

$$G_{Ndb} = 20 \log_{10} \frac{G_N}{G_{No}} \quad (A2.7)$$

$$G_{Ndb} = 20 \log_{10} G_N - 20 \log_{10} G_{No} \quad (A2.8)$$

Substituting (A2.4), (A2.6) into (A2.7)

$$G_{Ndb} = 20 \log_{10} \left( \frac{G_f}{G_{fo}} \right)^N = \frac{N}{3} \left\{ 20 \log_{10} \left( \frac{G_f}{G_{fo}} \right)^3 \right\}$$

Assume

$$G_{3db} = 20 \log_{10} \left( \frac{G_f}{G_{fo}} \right)^3 \quad (A2.9)$$

$$\text{So } G_{\text{Ndb}} = \frac{N}{3} G_{3\text{db}} \quad (\text{A2.10})$$

Substituting (A2.3), (A2.10) into (A2.8)

$$20 \log_{10} \frac{V_{\text{Nout}}}{V_{\text{in}}} = \frac{N}{3} G_{3\text{db}} + 20 \log_{10} G_{\text{No}} \quad (\text{A2.11})$$

$$\text{Assume } G_{\text{Nodb}} = 20 \log_{10} G_{\text{No}} \quad (\text{A2.12})$$

Substituting (A2.6) into (A2.12)

$$G_{\text{Nodb}} = 20 \log_{10} (G_{\text{fo}})^N G_{\text{i}} \quad (\text{A2.13})$$

Substituting (A2.12) into (A2.11)

$$V_{\text{in}} = \frac{V_{\text{Nout}}}{10^{\frac{1}{20} \left( \frac{N}{3} G_{3\text{db}} + G_{\text{Nodb}} \right)}} \quad (\text{A2.14})$$

$G_{\text{Nodb}}$  in equation (A2.13) is independent of circuit capacitance  $C$ . It can be found in the curves in Figure A2.1 that  $G_{3\text{db}}$  at  $f = 0$  for all curves start at  $G_{3\text{db}} = 0$ . It can be also explained as the circuit Figure 3.2(f) that when the circuit is working in dc no effect of by-pass and feedback for both  $C$  arises. The  $G_{\text{No}}$  is measured by experiment and listed in Table A2.1

Table A2.1 Calculated  $G_{\text{Nodb}}$  ( $N \leq 3$ )

N	1	2	3
$G_{\text{No}} = (G_{\text{fo}})^N \cdot G_{\text{i}}$	9.60	57.2	341
$G_{\text{Nodb}} = 20 \cdot \log_{10} G_{\text{No}}$ (dB)	19.64	35.14	50.6

Note: (1) Calculated:  $G_{\text{i}} = 1.64$  Experimental:  $G_{\text{i}} = 1.61$

$G_{\text{fo}} = 6$

$G_{\text{fo}} = 5.96$

(2) Experimental  $G_{\text{i}}, G_{\text{fo}}$  are used

Equation (A2.14) is used to calculate the component at the measured frequency.

From Table A2.1

$$G_{30\text{db}} = 50.6$$

when  $N = 3$  substituting  $G_{30\text{db}} = 50.6$  into equation (A2.14)

$$V_{\text{in}} = \frac{V_{3\text{out}}}{10^{\frac{1}{20}(G_{3\text{db}} + 50.6)}} \quad (\text{A2.15})$$

Example:  $V_{3\text{out}} = 0.109$  v. : output measured at third filter stage

$f = 3$  Hz : measured output frequency

$C = 1.0$   $\mu\text{F}$  : selected capacitor in Figure 3.2(f) for all three filter stages

We find  $G_{3\text{db}} = -0.64$  dB from  $C = 1.0$   $\mu\text{F}$  curve at  $f = 3$  Hz in Figure A2.1.

$$\text{so that } V_{\text{in}} = \frac{0.109}{10^{\frac{1}{20}(-0.64 + 50.6)}} = 0.346 \text{ mv}$$

(2) When  $N > 3$

In this case the attenuator,  $G_a$ , exists in the middle of filter, as indicated in Figure 3.1. The way of derivation is similar to that for  $N \leq 3$  except that the gain of attenuator has to be added.

$$\text{So } G_N = (G_f)^N \cdot G_i \cdot G_a \quad (\text{A2.16})$$

where  $G_a$  is the gain of the attenuator

$$G_{N_o} = (G_{f_o})^N \cdot G_{i_o} \cdot G_{a_o} = (G_{f_o})^N \cdot G_i \cdot G_a \quad (\text{A2.17})$$

where  $G_{a_o}$  is the gain  $G_a$  at  $f = 0$  and  $G_{a_o} = G_a$

Equations (A2.3), (A2.5) and (A2.7 - A2.11) are still applicable.

Substituting equation (A2.17) into (A2.12)

$$G_{\text{Noddb}} = 20 \log_{10} (G_{\text{fo}})^N \cdot G_i \cdot G_a \quad (\text{A2.18})$$

so that equation (A2.14) becomes

$$V_{\text{in}} = \frac{V_{\text{Nout}}}{10^{\frac{1}{20} \left( \frac{N}{3} G_{3\text{db}} + G_{\text{Noddb}} \right)}} \quad (\text{A2.19})$$

which is similar to equation (A2.14) except in the calculation of  $G_{\text{Noddb}}$ .

To calculate  $G_{\text{Noddb}}$ , equation (A2.18),  $G_a$  may be three selections  $G_{a1}$ ,  $G_{a2}$  and  $G_{a3}$  corresponding to switch K set in position  $a_1$ ,  $a_2$  and  $a_3$  respectively. The gains of  $G_{a1}$ ,  $G_{a2}$  and  $G_{a3}$  simply consist of the emitter follower of gain 1 and resistance divider, listed in Table 3.1 for actual resistor values. Therefore,  $G_{\text{Noddb}}$  is obtainable through calculation of equation (A2.18) and listed in Table A2.2.

Table A2.2 Calculated  $G_{\text{Noddb}}$  ( $N > 3$ )

	N=4			N=5			N=6		
	$G_{a1}$	$G_{a2}$	$G_{a3}$	$G_{a1}$	$G_{a2}$	$G_{a3}$	$G_{a1}$	$G_{a2}$	$G_{a3}$
	1	1/7.4	1/206	1	1/7.4	1/206	1	1/7.4	1/206
$G_{\text{No}} = G_i G_a^N G_{\text{fo}}$	2031	274	9.81	12106	1636	58.5	72157	9751	350
$G_{\text{Noddb}} = 20 \cdot \log_{10} G_{\text{No}}$	66.15	48.75	19.8	81.7	64.2	35.4	97.16	79.8	50.9

Note : Experimental  $G_i = 1.61$ ,  $G_{\text{fo}} = 5.96$  are used

The procedue to calculate the  $V_{\text{in}}$  with  $N > 3$  through equation

(A2.14) is similar to that used for  $N \leq 3$